

A. Murari, T. Edlington, J. Brzozowski, E. de La Luna, P. Andrew, G. Arnoux,
F.E. Cecil, L. Cupido, D. Darrow, V. Kiptily, J. Fessey, E. Gauthier,
S.Hacquin, K. Hill, A. Huber, T. Loarer, K. McCormick, M.Reich
and JET-EFDA contributors

JET New Diagnostic Capability on the Route to ITER

“This document is intended for publication in the open literature. It is made available on the understanding that it may not be further circulated and extracts or references may not be published prior to publication of the original when applicable, or without the consent of the Publications Officer, EFDA, Culham Science Centre, Abingdon, Oxon, OX14 3DB, UK.”

“Enquiries about Copyright and reproduction should be addressed to the Publications Officer, EFDA, Culham Science Centre, Abingdon, Oxon, OX14 3DB, UK.”

JET New Diagnostic Capability on the Route to ITER

A. Murari¹, T. Edlington², J. Brzozowski³, E. de La Luna⁴, P. Andrew², G. Arnoux⁵,
F.E. Cecil⁶, L. Cupido⁷, D. Darrow⁸, V. Kiptily², J. Fessey², E. Gauthier⁵,
S. Hacquin⁷, K. Hill⁸, A. Huber⁹, T. Loarer⁵, K. McCormick¹⁰, M. Reich¹
and JET-EFDA contributors*

¹Associazione EURATOM-ENEA per la Fusione, Consorzio RFX, 4-35127 Padova, Italy

²EURATOM/UKAEA Fusion Association, Culham Science Centre, Abingdon, UK

³Alfvén Laboratory, KTH, EURATOM-VR Association, Sweden

⁴Asociación EURATOM-CIEMAT para Fusión, CIEMAT, Madrid, Spain

⁵Association EURATOM-CEA, CEA Cadarache, 13108 Saint-Paul-lez-Durance, France

⁶Colorado School of Mines, 1500 Illinois St., Golden, Colorado

⁷CFN, Associacao IST/EURATOM, 1049-001 Lisboa, Portugal

⁸Princeton Plasma Physics Laboratory, P.O. Box 451, Princeton, New Jersey

⁹Institut für Plasmaphysik, Forschungszentrum Jülich, Association EURATOM-FZJ,
Trilateral Euregio Cluster, Germany

¹¹Max-Planck Institut fuer Plasmaphysik, EURATOM-Association, Boltzmannstr. 2, 85748 Garching, Germany

* See annex of J. Pamela et al, "Overview of JET Results",

(Proc. 20th IAEA Fusion Energy Conference, Vilamoura, Portugal (2004)).

Preprint of Paper to be submitted for publication in Proceedings of the
SOFT Conference,

(Warsaw, Poland 11th – 15th September 2006)

ABSTRACT

The JET scientific programme is directed towards the development of ITER relevant scenarios. In support of this, significant effort has been made to develop diagnostics to better characterise the power deposition on the plasma facing components, to investigate in more detail the radiation losses particularly in the divertor region and to better detect the MHD instabilities and their effects on the fast ion confinement. A new wide angle infrared camera provides for the first time the opportunity to perform infrared thermography in the JET main chamber, even during fast events like ELMs and disruptions. A completely new bolometric system, with better spatial resolution particularly in the divertor, is now used to investigate the total radiation losses and their influence on the ELM behaviour. A new set of microwave waveguides has improved by 20 dB the signal to noise ratio of the JET X-mode reflectometers, that are now routinely used to detect MHD instabilities and in particular to localise the location of the Alfvén Eigenmodes. This improved diagnostic capability to monitor MHD instabilities is complemented by two new diagnostics to detect lost fast particles. Both the new scintillator probe and a poloidal array of Faraday cups have already shown clear correlations between the MHD activity and the ion losses at the edge.

1. INTRODUCTION

Recent JET diagnostic upgrades have been driven by the main scientific programme, which is now aimed primarily at developing plasma scenarios for ITER. To this end diagnostic enhancements have concentrated in particular on improved determination of the plasma wall interactions, better measurement of the radiation losses and MHD instabilities, as well as on the detection of the fusion products. A new infrared wide-angle camera is specifically devoted to the study of power loads on the machine first wall (see section two). The emitted radiation can be studied now with a new bolometric tomography, with a much better spatial resolution particularly in the divertor region (see section three). In the field of plasma instabilities, a new array of corrugated transmission lines with reduced microwave losses were installed last autumn, providing a 20 dB increase in the signal to noise ratio of existing X-mode reflectometers. This consequent improvement in the quality of the measurements has allowed a more detailed characterization of MHD instabilities in general and of the Alfvén cascades in particular (see section four). JET also offers a unique environment for the development and testing of relevant “burning plasma” diagnostics. To alleviate a recognized weakness of JET diagnostic capabilities, two new systems for detecting the lost alphas were installed during the last shutdown. They consist of a poloidal array of Faraday cups and an in vessel scintillator probe (see section five). With these new instruments, it is possible to investigate the dependence of the fast ion losses from different heating schemes and magnetic configurations and to investigate correlations between the losses and plasma MHD activity. Future prospects of diagnostic upgrades at JET are summarized in section six.

2. PLASMA-WALL INTERACTIONS: IR THERMOGRAPHY

The capability of present day materials to withstand the power loads induced by thermonuclear plasmas remains one of the major issues on the route to a fusion reactor. This problem, which will be very significant in ITER, is already felt at JET in the present configuration of the machine and will be aggravated with the installation of the new Be wall and W divertor and by upgrades to the present heating systems. At JET it was therefore decided to develop a new infrared thermography diagnostic to determine the surface temperature of the plasma facing components in the main chamber and in the divertor.

A dedicated endoscope providing a wide-angle view (field of view of 70 degrees) in the infrared range (3.5 to 5 μ m) was installed during the last shutdown to perform thermography of the main chamber and divertor. The diagnostic consists of an endoscope formed by a tube holding the front head mirrors, a Cassegrain telescope, and a relay group of lenses, the latter being connected to the camera body [1]. To increase the ITER-relevance of the project, mainly reflective optical components were chosen, since they are the only kind which can sustain high neutron radiation. Thanks to the gold coating, the reflection on the front end mirrors is close to 98% and, taking into account the absorption of the lenses, the global transmission of the endoscope is higher than 60%. The diagnostic is designed to measure from the JET operating temperature of 200 $^{\circ}$ C up to a maximum temperature of 2000 $^{\circ}$ C. The diagnostic spatial resolution is diffraction limited as determined by off-line measurements based on the Modulation Transfer Function (MTF) technique. Since the temperature measurements require an absolute determination of the photon flux, assuming a 10% error in this quantity, an overall spatial resolution of 2 cm at three meters was estimated. A frame rate of 100 Hz at full image size can be achieved and it can be increased up to 10 kHz by reducing the image size to 128x8 pixels, located at any position in the field of view.

With this new diagnostic it is possible now for the first time to perform detailed thermography measurements in JET main chamber. The system has the potential to provide new information on the power losses also during transient events, like ELMs and disruptions, which are a particular concern for ITER. In figure 1 the power deposition losses induced by a disruption with a Vertical Displacement Event (VDE) are clearly seen to affect the top of the vacuum vessel. This disruption was characterised by: 0.5MJ Thermal Energy losses, 1.2 MJ Mag Energy losses. Only 0.6 MJ were radiated and 1.4 MJ conducted to ceiling tiles, causing a peak of the surface temperature of 600 $^{\circ}$ C. The losses induced by a type I ELM are shown in figure 2. In the main chamber the most affected regions are on the low field side above the equatorial plane. Preliminary evaluations seem to indicate that 0.2 MJ ELMs can easily induce an increase in the temperature of these hot spots up to at least 800 $^{\circ}$ C.

3. EMITTED RADIATION: BOLOMETRY

One of the main differences between present day machines and ITER is certainly the fraction of radiated power. ITER reference scenarios are supposed to be about 90% radiative, in order to reduce the peak power loads, whereas at JET normal discharges have a radiated fraction of the order of 50%.

Moreover the radiated fraction and the spatial distribution of the radiated power can strongly influence the behaviour of the ELMs, another crucial factor for the lifetime of the plasma facing components. In JET a new bolometric system was designed and installed during the last shutdown in order to improve the determination of the emitted radiation [2]. This was achieved mainly by increasing the coverage of the plasma cross section and the spatial resolution particularly in the divertor. The new bolometric tomography consists of two cameras (at different octants), one viewing vertically and one horizontally, as shown in figure 3. The vertical camera has 16 channels with a separation between 13 and 25 cm in the mid-plane; they are complemented by 8 channels specifically devoted to the divertor with a separation of 8 cm between the various lines of sight (at the top of the divertor). The horizontal camera comprises 4 upper channels (vertical separation ~ 15 cm at $R = 3$ m), 12 middle channels (separation 18-22cm) and 8 lower channels for the divertor (separation ~ 8 cm). The two cameras are complemented by a series of bolometers located in the divertor. The detectors are gold metal foil bolometers with mica insulators which, together with their dedicated electronics, provide a temporal resolution of 2ms, a sensitivity of 6.2V/W and an energy range up to 8 keV. The estimated lowest detectable signal is of the order of 2mW/cm^2 . With this new instrument, tomographic reconstructions of the total radiated power can be performed with high temporal and spatial resolution. A typical example is shown in figure 4, where the radiation pattern in the divertor during and between ELMs is resolved in good detail, proving the quality of the measurements at high time resolution.

4. MHD INSTABILITIES: REFLECTOMETRY

In tokamak plasmas, tearing-like Magneto Hydrodynamic Modes (MHD) can develop on or near q -rational surfaces. These instabilities are traditionally diagnosed with the help of magnetic pick-up coils near the plasma boundary but, since they affect the density profile, mainly flattening it locally, they can be detected by measuring the local electron density fluctuations. On JET, high frequency MHD modes have been studied by measuring the density perturbations they induce. Various classes of Alfvén eigenmodes, destabilized by energetic ions in reversed shear plasmas such as Alfvén Cascades (AC), were diagnosed by using an O-mode reflectometer operating in the interferometric regime as a microwave refractometer [3]. With this approach, supported also by the fluctuations in the FIR interferometer line integrated density measurements, it was possible to monitor the evolution of the minimum safety factor. Unfortunately a drawback of both the interferometer and refractometric approaches is that they cannot give any information about the spatial localisation of the modes. To overcome this limitation, X-mode reflectometric measurements are an obvious alternative but in the past reflectometer measurements at JET were restricted by the very high losses in the over-size waveguides. To alleviate this problem, a new array of wave guides was installed during the last shutdown. It consists of four circular, internally corrugated waveguides for the reflectometric measurements and two smooth walled waveguides for the ECE oblique viewing. The implementation of this new hardware allows reduction in the losses in the reflectometric channels of about 20dB, rendering feasible a complete new series of physical studies. A typical example of reflectometry

measurement of density fluctuations associated with Alfvén cascades is illustrated in figure 5. The spectrogram (sliding FFT) of the reflected signal is reported, which allows the time-frequency determination of the Alfvén cascades with particularly high resolution. Modes with a n number up to 16 have already been identified and, with the maximum acquisition rate of 1 MHz, a time resolution of 1ms can be easily achieved.

5. BURNING PLASMA: LOST ALPHA PARTICLE DIAGNOSTICS

One of the main objectives of the next generation of fusion devices like ITER is to study the confinement of energetic particles (fast ions from auxiliary heating and fusion born alpha particles). On JET the field of fast particle physics is becoming particularly relevant with the near installation of the new ITER-like ICRH antenna. In order to investigate fast particle losses, it was therefore decided to install two new diagnostics explicitly devoted to this purpose; a scintillator probe and an array of Faraday cups. The principle of the scintillator probe is based on imaging the lost particles with a suitable scintillator located close to the plasma edge. With the design of a proper collimator, a wide range of energies and pitch angles can be covered.

The collimator of the JET scintillator probe was optimised with the orbit-tracing Monte-Carlo code *efipdesign*' [4] to select particles with Larmor radii from 4 to 13cm and pitch angles between 34 and 86 degrees. Since the detector is located close to the Neutral Beam injector, a gold foil (1mm) was located behind the entrance aperture to block the prompt losses of low energy (below 200keV) hydrogen isotopes. As scintillator material P56 ($Y_2O_3:Eu_3$) was chosen for its high photon rate per incident ion (compared to P46 and P43) and high life-expectancy. The main drawback of this material is the relatively long decay time of about 2ms, which limits the time resolution to timescales above a few milliseconds. The emission from the scintillator plate is relayed by a set of lenses onto a coherent fibre optics bundle, which images it at the cold end of the diagnostic on a frame-transfer (no dead time) CCD camera (RoperScientific Cascade 512B) and on a Hamamatsu 4×4 photomultiplier tube array (a cube beam splitter is inserted to split the image). The CCD camera can achieve a maximum time-resolution of 20Hz, with the full spatial resolution provided by the fibre bundle (95×36). The correlation between the fast particle losses and sawteeth and tornado modes is reported in figure 6. The losses are in general higher and more peaked in both energy and pitch angle for the case of ELMs.

The Faraday cups are stacks of metallic foils separated from each other by an insulating material. Depending on its energy, a particle can pass through a certain number of foils before it is stopped in one. The charge collected by a foil generates a small current which can be measured. In the JET version of the diagnostic each detector consists of 4 $75\text{mm} \times 25\text{mm}$ Ni foils ($2.5\mu\text{m}$ thick in eight of the detectors and $1.0\mu\text{m}$ thick in the ninth) which are separated by insulating mica foils [5]. They were designed to detect the current of fast ions at multiple poloidal locations, with a dynamic range of $1\text{nA}/\text{cm}^2$ to $10\text{mA}/\text{cm}^2$. The detectable range of α -particle energies is about 1-5MeV and the temporal resolution is 1ms. The energy resolution for 3.5 MeV α -particles is estimated to be about 15-50%. The array consists of nine detectors distributed over five poloidal locations between $z = 22$ and 80cm

below the midplane. In the radial direction, the detectors are equally spaced on three locations between 25 and 85 mm behind the adjacent the poloidal limiter. The poloidal distribution of fast particle losses during ICRH is illustrated in figure 7. The losses are higher below the horizontal mid-plane, particularly at 21 and 27 degrees.

FUTURE PROSPECTS

JET long term programme includes an increase of the additional heating power and a completely new mechanical plasma boundary, with a Be wall and a W divertor. The main areas of future developments in diagnostics will be in the fields of spectroscopy, wall erosion and redeposition, diagnostics for the fusion products and real time.

REFERENCES

- [1]. E. Gauthier “*ITER-like wide-angle infrared thermography and visible observation diagnostic using reflective optics*” this conference
- [2]. A. Huber “*Upgrade of Bolometer System on JET for Improved radiation Measurements*” this conference
- [3]. S Sharapov et al, Physic Review Letters **93** 165001 (2004)
- [4]. S. Baemel S et al, Rev. of Sci. Instrum. **75**, 3563 (2004)
- [5]. D.S. Darrow, S. Baumel, F.E. Cecil, V. Kiptily, R. Ellis, L. Pedrick and A. Werner, Rev. Sci. Instrum. **75**, 3566 (2004).

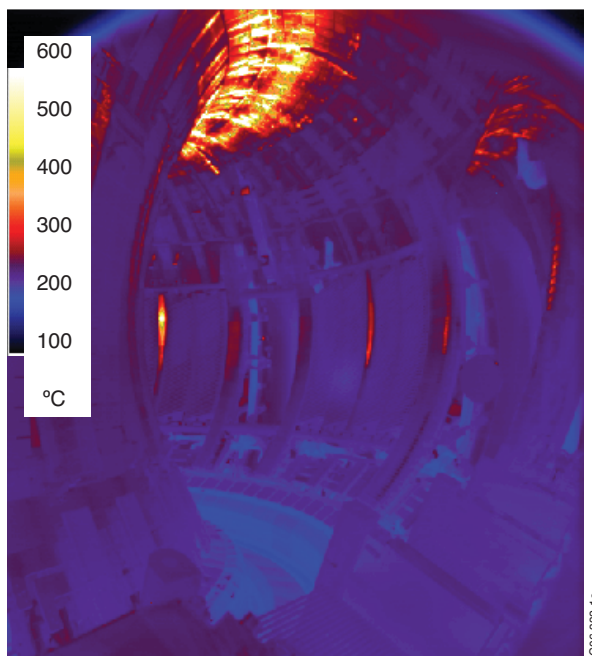


Figure 1: Thermographic image of JET main chamber obtained with the new IR wide angle camera during a disruption with a Vertical Displacement Even (Pulse No: 6398)

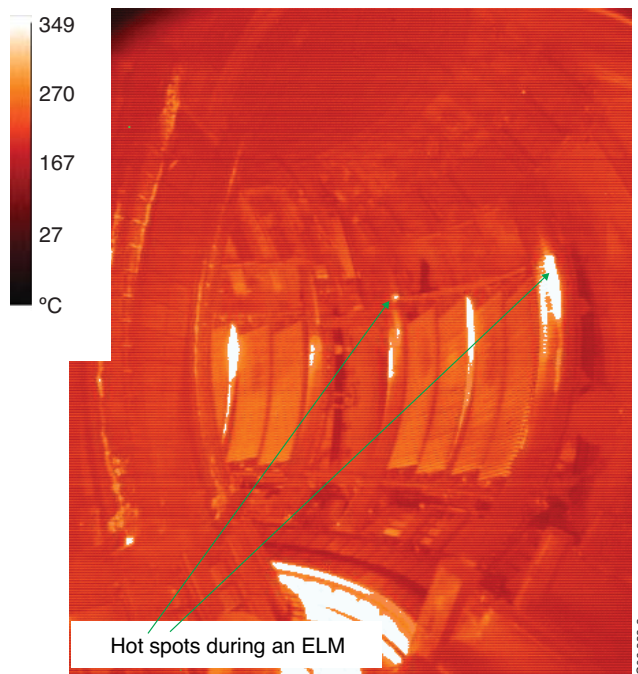


Figure 2: Thermographic image of JET main chamber obtained with the new IR wide angle camera during an ELM, showing some hot spots (Pulse No: 66231 $t=17.751$ frame rate =150Hz).

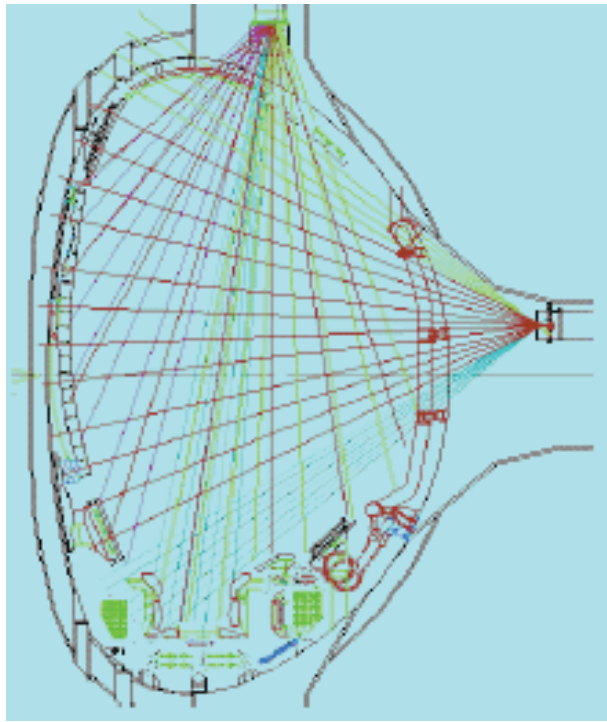


Figure 3: Lines of sight of JET new bolometric tomography.

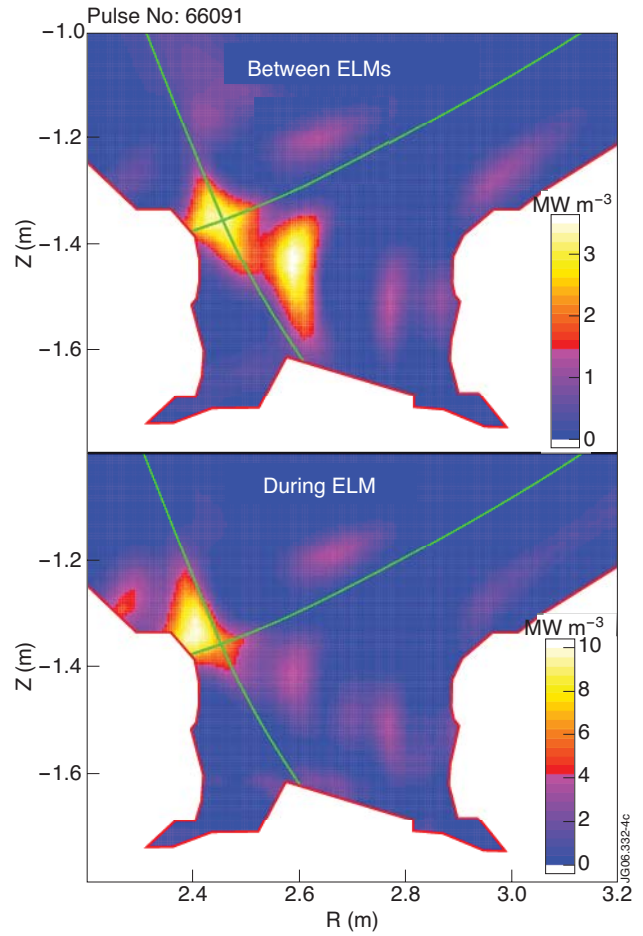


Figure 4: Tomographic reconstruction of the radiated power between ELMs and during one ELM for Pulse No: 66091. Integration time 10 ms

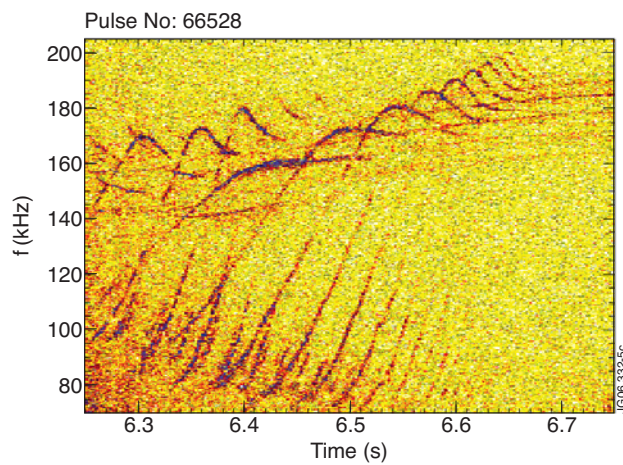


Figure 5: Spectrograms of the density fluctuations induced by the Alfvén cascades as detected with JET X-mode reflectometer (Pulse No: 66528, toroidal field $B_t=3.2T$, Xmode channel at 103 GHz reflected at about $R=3.1m$)

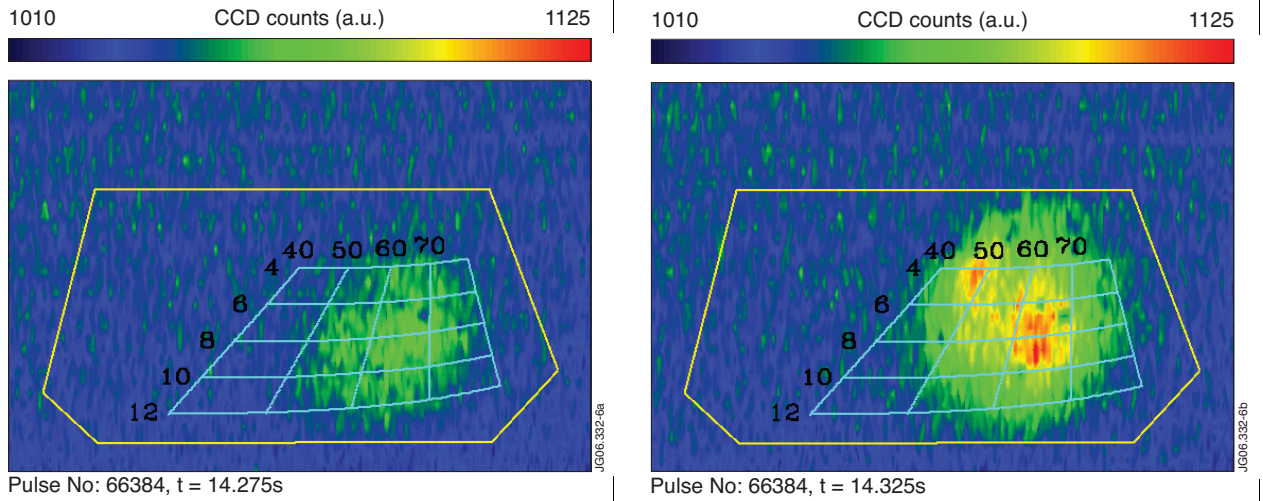


Figure 6: Emission of the scintillator probe due to tornado modes before a sawtooth crash (top) and after the crash (bottom).

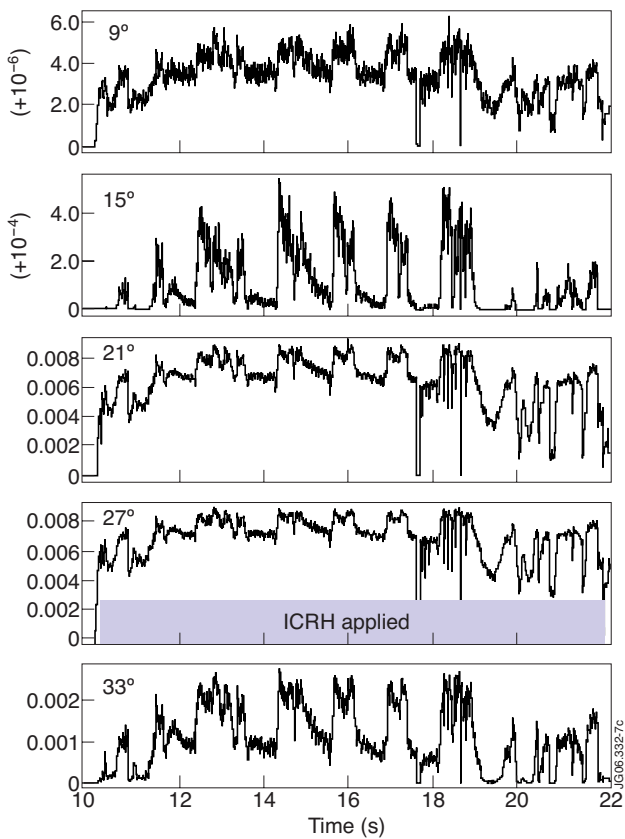


Figure 7: Poloidal distribution of fast particle losses during ICRH heating for JET Pulse No: 66209. The currents of various Faraday cups are plotted versus time. The angles are in the poloidal direction below the midplane on the low field side (reference is the midplane at zero degrees)